Angular Disinhibition Effect in a Modified Poggendorff Illusion

Yingwei Yu and Yoonsuck Choe
Department of Computer Science
Texas A&M University
3112 TAMU
College Station, Texas 77843-3112, USA
{yingwei,choe}@tamu.edu

Abstract

Visual illusion can be strengthened or weakened with the addition of extra visual elements. For example, in Poggendorff illusion, with an additional bar added, the illusory skew in the perceived angle can be enlarged or reduced. In this paper, we show that a nontrivial interaction between lateral inhibitory processes in the early visual system (i.e., *disinhibition*) can explain such enhancement or degradation of the illusory percept. The computational model we derived successfully predicted the perceived angle in a modified Poggendorff illusion task with an extra thick bar. The concept of disinhibition employed in the model is general enough that we expect it can be further extended to account for other classes of geometric illusions.
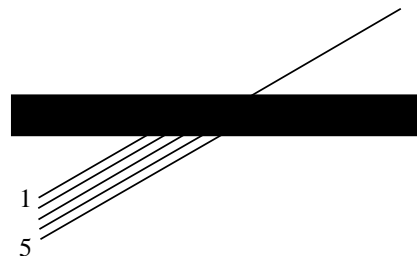
Figure 1: **The Poggendorff Illusion.** The original Poggendorff illusion is shown. The five lines below the horizontal bar are labeled 1 to 5 from top to bottom. Line 3 is physically collinear with the line on top. In this example, line 4 is perceived to be collinear.

Introduction

Visual illusions are important phenomena because of their potential to shed light on the underlying functional organization of the visual system. For simple illusions, a simplistic explanation can be sufficient, but when multiple effects exist in an illusion, the final percept can be quite complex. For example, when we perceive an angle, our perception of the angle is usually greater than the actual angle (*expansion* effect), but when there are multiple lines and thus multiple angles, the expansion effect can be either enhanced or reduced.

Such an interference effect can be demonstrated in a modified Poggendorff illusion. In the original Poggendorff illusion (see, e.g., Tolansky 1964; Morgan 1999), the top and the bottom portions of the penetrating thin line is perceived as misaligned (figure 1). Figure 2 shows how such a perception of misalignment can occur. The line on top forms an angle α with the horizontal bar, but the perceived angle α' is greater than α (i.e., exaggerated). As a result, the line on top is perceived to be collinear with line 4 on the bottom, instead of line 3 which is physically collinear. However, when an additional bar is added, the perceived illusory angular expansion effect is altered: the effect is either reduced (figure 3) or enhanced (figure 4) depending on the orientation of the newly added bar. Understanding the functional organization and the low-level neurophysiology underlying such a nontrivial interaction is the main aim of this paper.

Neurophysiologically speaking, in the original case where two orientations interact, lateral inhibition between orientation cells in the visual cortex can explain the enlargement in perceived angle. However, as we have seen in figures 3 and 4, when an additional orientation response is triggered, lateral inhibition alone cannot explain the complex effect. Our
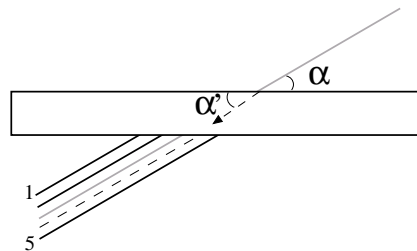
Figure 2: **The Angle Displacement in the Poggendorff Illusion.** The actual angle α ($= 30°$) and the perceived angle α' ($> 30°$) are shown. The gray line shows the straight line penetrating the bar. The dashed line below shows the perceived direction in which the line on top seemingly extends to.

observation is that this complex response is due to disinhibition, i.e., inhibition of another inhibitory factor resulting in effective excitation (Hartline et al. 1956; Hartline and Ratliff 1957, 1958; Stevens 1964; Brodie et al. 1978). Unlike simple lateral inhibition between two cells, we explicitly accounted for disinhibition in our computational model to describe the complex interactions between multiple orientation cells. The resulting model based on the neurophysiology of the early visual system was able to accurately predict the perceptual performance for the modified Poggendorff illusion.

The rest of the paper is organized as follows. First, a neurophysiological motivation for our computational model is presented, followed by a detailed mathematical description of the model. Next, the results from the computational experiments with the model is presented and compared to psychophysical data, followed by discussion and conclusion.
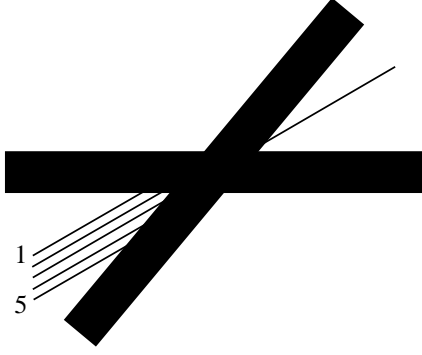
Figure 3: **The Poggendorff Illusion with an Additional Thick Bar of 50 °.** The Poggendorff figure with an additional bar at 50° is shown. In this case, line 2 is perceived to be collinear (i.e., $\alpha' < 30°$).
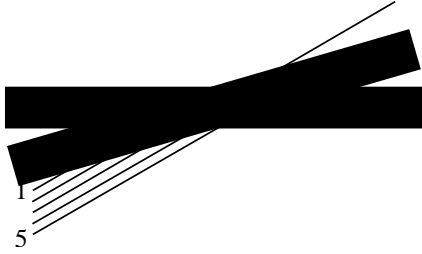

Figure 4: **The Poggendorff Illusion with An Additional Thick Bar of 20 °.** The Poggendorff figure with an additional bar at 20° is shown. For this case, unlike in figure 3, line 4 (or to some, line 5) is perceived to be collinear ($\alpha' > 30°$). (The α' in this case is slightly greater than in original Poggendorff figure.)

Computational Model of Disinhibition in the Visual Cortex

Let us first consider how orientation columns in the visual cortex interact in response to several intersecting lines. For each line at the intersection, there are corresponding orientation columns that respond maximally, with a Gaussian response distribution. As multiple simple cells are activated by the different lines at the intersection, the response levels will interact with each other through lateral connections. Thus, there are two issues we want to more precisely address: (1) what exactly is the activation profile (or the response distribution) of the orientation-tuned cells, and (2) how these cells interact with each other through the lateral connections.

The Activation Profile of Orientation Columns

Each simple cell in the primary visual cortex responds maximally to visual stimuli with a particular orientation. The response of these cells to different orientations can be modeled as a Gaussian function:

$$y = y_0 + \frac{A}{\sigma\sqrt{\pi/2}}\exp(-2\frac{(x-x_c)^2}{\sigma^2}), \qquad (1)$$

where y_0 is an offset; x_c is the center (or mean); σ is the standard deviation; and A is a scaling constant (Martinez et al. 2002).

It also comes to our attention that the cell tuned for a certain orientation, say α, should respond to the opposite orientation, which is $\alpha + 180°$. However, experiments have shown that the peak at the position $\alpha+180°$ is somewhat smaller than the peak at α (Alonso and Martinez 1998). To accurately model this, we need two Gaussian curves to fit the responses of a cell to a full range of orientations from $-180°$ to $180°$.

The fitting curve can be written as follows:

$$
\begin{aligned}
y \quad = \quad & y_0 \\
+ \quad & \frac{A}{\sigma\sqrt{\pi/2}}\exp(-2\frac{(x-x_c)^2}{\sigma^2}) \\
+ \quad & \frac{AK}{\sigma\sqrt{\pi/2}}\exp(-2\frac{(x-x_c+\pi)^2}{\sigma^2}), \qquad (2)
\end{aligned}
$$

where K is the rate of activation for the opposed direction ($K < 1$). Such an asymmetric response enables the the simple cells to be sensitive to the direction (as well as orientation).

Using the equation, we can now visualize the response profile of simple cells tuned to orientations ranging from 0 to 360°. Figure 5 shows the responses of orientation columns tuned to -90°to 270° (x-axis) to inputs of two different orientations, 0 and 30°. Figure 6 shows the responses of the same set of orientation columns to inputs of two orientations of 0 and 150°. From these two figures, we can observe that for each specific orientation input, the excitation is tuned at that value with a peak in the Gaussian curve, and at the same time, the opposite orientation tuned cell shows a lower peak response. The asymmetry in responses occur in both an acute angle (figure 5) and an obtuse angle (figure 6). Note that even though the difference in orientation between 0° vs. 30° and 0° vs. 150° is 30° in both cases, the response profile greatly differs in the 0° vs. 150°case.

This is an improvement over conventional excitation profile models such as Gabor filters (Daugman 1980), which make no distinction between these two angles in the two figures. Using the more accurate response profile, we will next investigate how these response profiles can interact.

Column Level Inhibition and Disinhibition

Our observation that the angular enlargement sometimes seems to be weakened when there are more than two bars or lines in the Poggendorff illusion (figure 3) led us to hypothesize about the potential role of a recurrent inhibition effect, i.e., disinhibition. Basically disinhibition is the inhibition on other inhibitory factors, resulting in a net excitatory effect at the target. Experiments on the Limulus (horseshoe crab) optical cells showed that the final response of each receptor resulting from a light stimulus can be enhanced or reduced due to the interactions through inhibition from its neighbors. Note that disinhibition has also been found in vertebrate retinas such as in tiger salamanders (Roska et al. 1998) and in mice (Frech et al. 2001). In the following, the Limulus neurophysiology giving rise to disinhibition is summarized, followed by the description of our computational model based on the Limulus model.

Hartline-Ratliff's model of disinhibition Experiments on Limulus optical cells have shown that lateral inhibition effect
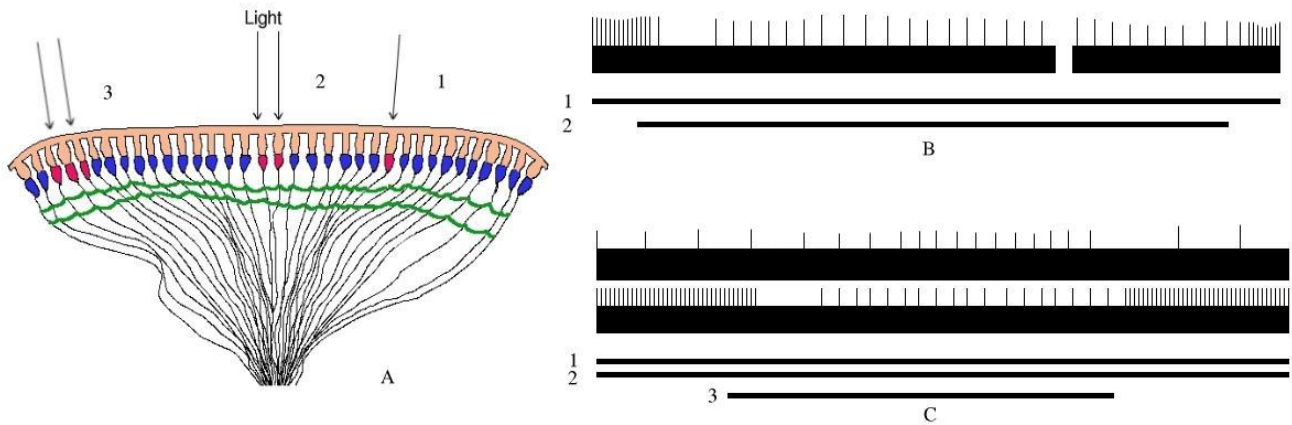
Figure 7: **Lateral inhibition in Limulus optical cells.** The figure shows the disinhibition effect in Limulus optical cells. (*a*) The retina of Limulus. Point light is presented to three locations (1, 2 and 3). (*b*) The result of lighting position 1 and 2. The top trace shows the spike train of the neuron at 1, and the two bars below show the duration of stimulation to cell 1 and 2. When position 2 is excited, the neuron response of position 1 gets inhibited. (*c*) Both 1 and 2 are illuminated, and after a short time, position 3 is lighted. The top two traces show the spike trains of cell 1 and cell 2. The three bars below are input duration to the three cells. As demonstrated in the figure, when position 3 is lighted, neurons at position 2 get inhibited by 3, so its ability to inhibit others get reduced. As a result, the firing rate of neuron at position 1 gets increased during the time neuron at position 3 is excited. This effect is called disinhibition. Redrawn from (Hartline and Ratliff 1957).
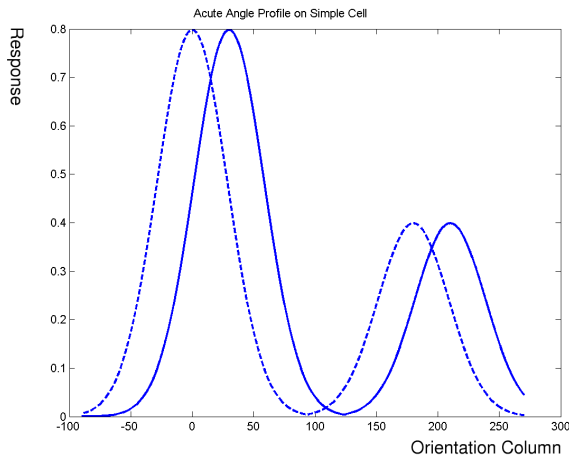

Figure 5: **The Activation on Simple Cell by an Acute Angle** (30°)**.** The dotted curve is the responses of the orientation columns (x-axis) to a horizontal line of 0°, and the solid curve is the responses to 30° line.
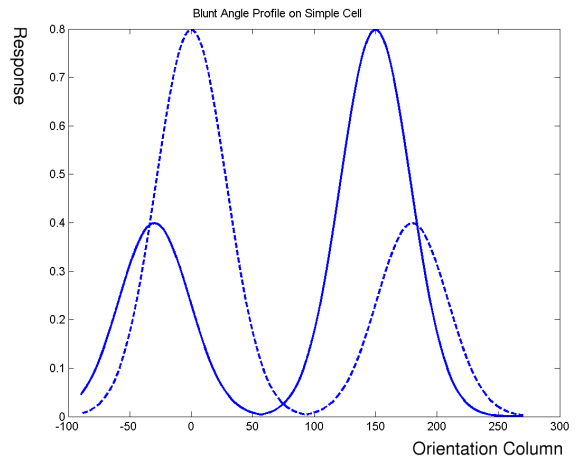

Figure 6: **The Activation on Simple Cell by Blunt Angle.** The dotted curve is the responses of the orientation columns (x-axis) to a horizontal line of 0°, while the solid curve is the responses to a 150° line.

is recurrent (figure 7; see Hartline and Ratliff 1957, 1958). The final response of a specific neuron can be considered as the overall effect of the response from itself and from all other neurons. Conventional convolution operation using lateral inhibition alone does not account for the effect of disinhibition which plays an important role in the final response. The final response of each receptor resulting from a light stimulus can be enhanced or reduced due to the interactions through inhibition from its neighbors, which may be important. (Such disinhibition effects have been found to play an important role in brightness-contrast illusions Yu et al. (2004).)

Hartline and his colleagues also did significant mathematical modeling of the Limulus optical cell response. The Hartline-Ratliff equation describing disinhibition in the Limulus can be written as follows (Hartline and Ratliff 1957, 1958; Stevens 1964):

$$r_m = \epsilon_m - K_s r_m - \sum w_{m \leftarrow n}(r_n - t_{m \leftarrow n}), \quad (3)$$

where r_m is the response, K_s is the self-inhibition constant, ϵ_m is the excitation of the m-th ommatidium, $w_{m \leftarrow n}$ is the inhibitory weight from other ommatidia, and $t_{m \leftarrow n}$ the threshold.

Brodie et al. extended this equation to derive a spatiotemporal filter, where the input was assumed to be a sinusoidal grating (Brodie et al. 1978). This model is perfect in predicting Limulus retina experiments as only a single spatial frequency channel filter, which means that only a fixed spatial frequency input is allowed (Brodie et al. 1978). Because

of this reason, their model cannot be applied to a complex image, as various spatial frequencies could coexist in the input. In the following section, we will build upon the Hartline-Ratliff equation and derive a filter that can be used in modeling orientation columns.

A simplified model of disinhibition   Based on the Hartline-Ratliff equation above, we derived a model for two-dimensional disinhibition as follows (Yu et al. 2004):

$$\mathbf{r} = W^{-1} \times \mathbf{x}. \tag{4}$$

where $\mathbf{r}$ is the output vector, $\mathbf{x}$ is the input vector and W is the weight matrix:

$$W_{ij} = \begin{cases} -w(|i,j|) & \text{when } i \neq j \\ \\ 1 & \text{when } i = j \end{cases}, \tag{5}$$

where $w(i,j)$ is the kernel function (usually a difference-of-Gaussian) defining the inhibition rate from the j-th neuron to the i-th neuron. Based on this simplified model of disinhibition, we can now more easily derive the disinhibition effect at the orientation column level.

Applying disinhibition to orientation cells   Cells occupying the same single orientation column in the cat visual cortex are known to inhibit each other (Blakemore and Tobin 1972). From this, we can postulate that a group of cells tuned to the same orientation representing different lines (e.g., intersecting lines) may compete with each other through inhibition.

Now let us consider the mathematical description for the inhibition at the column level. Suppose a group of orientation cells tuned to orientation α receives n lines as their inputs. The initial excitation $E_{\alpha i}$ for a cell inside this group α can be calculated as follows:

$$\begin{aligned} E_{\alpha i} &= y_0 \\ &+ \frac{A}{\sigma\sqrt{\pi/2}}\exp(-2\frac{(\alpha - x_c(i))^2}{\sigma^2}) \\ &+ \frac{AK}{\sigma\sqrt{\pi/2}}\exp(-2\frac{(\alpha - x_c(i) + \pi)^2}{\sigma^2}), \end{aligned} \tag{6}$$

where y_0 is an offset, A is a scaling constant for the Gaussians, σ is the standard deviation, K is the rate of activation of the opposite direction, and $x_c(i)$ is the orientation of the i-th input line. In this way, we can calculate the excitation E of the cell to the i-th line on a certain group of cells tuned to α. All those parameters in this equation are fairly standard parameters, which does not require a precise tuning.

Using the Hartline-Ratliff equation (Hartline and Ratliff 1957) for recurrent lateral inhibition and the simplified model of disinhibition (Yu et al. 2004), the final response R of cell i in orientation column α can be obtained as follows:

$$R_{\alpha i} = E_{\alpha i} - W \times R_{\alpha i}, \tag{7}$$

where W is a constant matrix of inhibition rate (or weight, controlled by a free parameter η: $w_{ij} = \eta$ if $i \neq j$, and

0 otherwise). From this, we can finally derive the response equation which accounts for the disinhibition effect:

$$R_{\alpha i} = (I - W)^{-1} \times E_{\alpha i}, \tag{8}$$

where I is the identity matrix.

By applying the orientation α to all the columns, the projection of each line to the columns should shift a little bit depending on the strength of the activation of each line. Thus, the final perceived line orientation γ can be obtained by finding the maximum response after the inhibition process:

$$\gamma_i = \mathrm{argmax}_{\alpha \in C} R_{\alpha i} \tag{9}$$

where γ_i is the perceived orientation for the i-th line, R is the responses of i-th neuron tuned to orientation α and C is the set of all the orientation columns in layer 4 of the visual cortex.

Experiments and Results

Prediction of Angle Expansion without Additional Context

To test the model in the simplest stimulus configuration, we used stimuli consisting of one thick bar and one thin line. The thick bar was fixed at $0°$, and the thin line was rotated to various orientations while the perceived angle was measured in the model. The enlargement effect of the angle varied depending on the orientation of the thin line. As shown in figure 8, we can observe that there are three major characteristics of this varying effect. First, for the acute angles, there is an increment in the angle of the perceived compared to actual, but for the obtuse angles, the perceived angle is less than the actual angle. Second, the peak is around $20°$ for the largest positive displacement, and around $160°$ for the largest negative displacement. Third, there is an obvious asymmetry in the displacements between the acute angles and the obtuse angles. Note that the peak at $20°$ is greater in magnitude than the dip at $160°$. As compared in figure 8, these results are consistent with results obtained in psychophysical experiment by Blakemore et al. (1970).

Prediction for the Modified Poggendorff Illusion

Disinhibition effect is the key observation leading to our extension to the angular expansion model based on lateral inhibition alone. Because of disinhibition, when more than two lines or bars intersect, the perceived angle of the thin line will deviate from the case where only two lines or bars are present. Figure 9 shows the prediction of our model (solid line) when a second thick bar of varying orientations was added to the original Poggendorff illusion (see figure 3 and 4 for an example). If disinhibition effect did not exist, the solid line would have come out flat, however, there is an interesting peak and a valley in the predicted response. The effect demonstrated in figure 3 is accurately predicted by the peak near $20°$, and the effect in figure 4 by the valley near $50°$. So, at least for these two cases, we can say that our disinhibition-based explanation is accurate. However, does the explanation hold for an arbitrary orientation? To test this, we conducted a psychophysical experiment to measure human perceptual performance and compare the results to the model prediction (the results are shown as data points in figure 9).
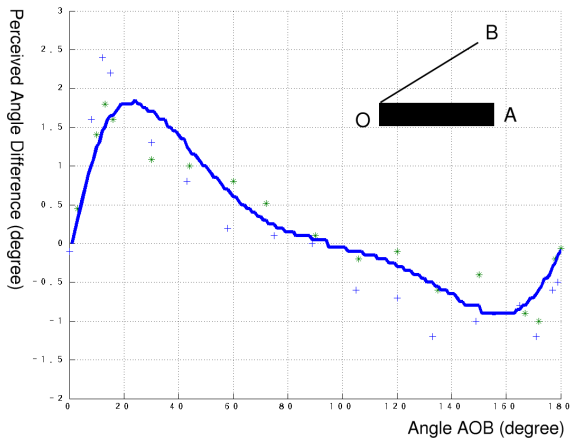
Figure 8: **The Variations of Perceived Angle Between Two Intersecting Lines.** The x-axis corresponds to the angle $\angle AOB$ (inset), from 0 to 180°. The y-axis is the difference between the perceived angle and the actual angle. The solid line is the result predicted by our model, and the data points * and + are data from human subjects in Blakemore et al. (1970). The curve was generated in two iterations, with the following parameters: $\eta = 0.009$ and $\sigma = 1.0$ for the first pass; $\eta = 0.005$ and $\sigma = 0.5$ for the second. The other parameters remained the same for both iterations: $y_0 = 0.0$ and $K = 0.5$.

Figure 9: **Perceived Angle in a Modified Poggendorff Illusion.** The results from the computational model (solid line) and human experiments (data points marked * and +) on a modified Poggendorff illusion (figure 3) are plotted. The second thick bar was rotated while the perceived angle was measured. The x-axis indicates the angle of the second bar. The y-axis shows the perceived angle of the thin 30° line. The model prediction and the human data are in close agreement. The parameters used in this experiment were as follows: free parameter: $\eta = 0.02$; standard parameters: $y_0 = 0$, $\sigma = 0.5$, and $K = 0.5$.

Experimental methods Two subjects with normal vision participated in the experiment (the authors YC and YY). An LCD panel with a 1024×768 resolution, which is supposed to be high enough to avoid line aliasing artifacts, was used to display the stimuli. The computer program displayed two thick bars and one thin line on the screen, similar to the stimulus in figure 3. The first thick bar was fixed in the center of the screen at 0°, and the width was 100 pixels. The thin line, 5 pixels in width, intersected the horizontal bar at a fixed angle of 30°. The second thick bar, 100 pixels in width, intersected at the same point as the the other two, where as the angle was varied from trial to trial. The program also displayed up to 10 thin lines (all 30°) below the horizontal bar, from which the subjects were asked to choose the one that is the most collinear to the thin line above the bar. The subject was allowed to click on the line of choice, and the perceived angle was recorded for each click, and a new stimulus was generated. A total of 101 trials were recorded for each subject.

Results Figure 9 shows the result of the psychophysical experiment (data points * and + for YC and YY, respectively), along with the prediction of the model (solid line). The peak (near 20°) and valley (near 50°) are apparent in the experimental data, and the overall shape of the curve closely agrees with the model prediction. The results show that our model of angular interaction based on disinhibition can accurately explain the modified Poggendorff illusion, and that low-level neurophysiology can provide us with insights into understanding the mechanisms underlying various visual illusions. Note that for this experiment, our disinhibition model is more comprehensive than the calculation method of simply summing up two Poggendorff effects by two separate bars. First it is because disinhibition is the summing up between all
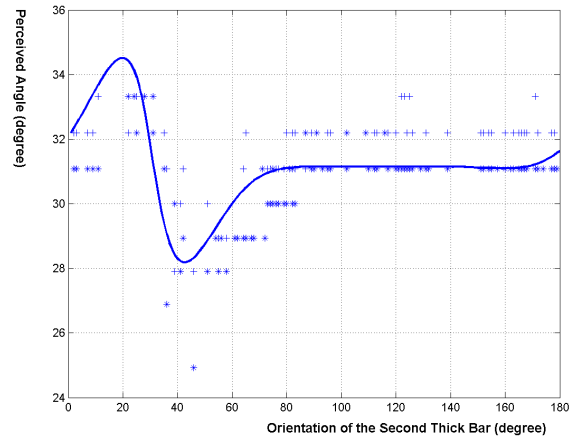
the pairs of bars at neuronal level, and second, simply summing up the effects of two bars omits the interactions between the lateral inhibition effects.

Discussion

We have presented a model based on angular inhibition by considering the disinhibition effect. The soundness of the theoretical extension lies in the fact that it is grounded in physiological and psychological facts. First, at the cellular level, lateral inhibition and disinhibition effects are found in the visual column of cat (Hubel and Wiesel 1962; Blakemore and Tobin 1972) and it is known that the opposite directions of the same orientation evoke an asymmetric response (Alonso and Martinez 1998). Our prediction of the angle variations for acute and obtuse angles shows asymmetric properties and matches these experiments. Second, our model can correctly predict the disinhibition caused by more than two lines intersected and the results match with our own experimental observation using the same kind of stimuli.

Besides the Poggendorff illusion, our model has the potential for explaining other geometric illusions, such as the café-wall illusion. Fermüller and Malm (2003) showed a variation of the café-wall illusion where adding some dots in strategic places significantly reduced the perceived distortion. Such a correctional effect can be explained by our model. Because the newly introduced dots give rise to a new orientation component (as the second thick bar did in our modified Poggendorff illusion), the disinhibitory effect caused by that new orientation can reduce the distortion formed by the existing orientation components.

Even though the disinhibition model presented in this paper is largely motivated by low-level neurophysiology, disinhibition can potentially serve a more general function. For ex-

ample, disinhibition can also be applied to higher brain functions such as categorization and memory (see Vogel (2001) for a model of associative memory based on disinhibition).

Conclusion

In this paper, we presented a neurophysiologically based model of disinhibition to account for a modified version of the Poggendorff illusion. The model was able to accurately predict a subtle orientation interaction effect, closely matching the psychophysical data we collected. We expect the model to be general enough to account for other kinds of geometrical illusions as well.

Acknowledgment

References

Alonso, J., and Martinez, L. M. (1998). Functional connectivity between simple cells and complex cells in cat striate cortex. *Nature neuroscience*.

Blakemore, C., Carpenter, R. H., and Georgeson, M. A. (1970). Lateral inhibition between orientation detectors in the human visual system. *Nature*.

Blakemore, C., and Tobin, E. A. (1972). Lateral inhibition between orientation detectors in the cat's visual cortex. *Exp. Brain Res.*

Brodie, S., Knight, B. W., and Ratliff, F. (1978). The spatiotemporal transfer function of the limulus lateral eye. *Journal of General Physiology*, 72:161–202.

Daugman, J. G. (1980). Two-dimensional spectral analysis of cortical receptive field profiles. *Vision Research*, 20:847–856.

Fermüller, C., and Malm, H. (2003). Uncertainty in visual processes predicts geometrical optical illusions. *Vision Research*.

Frech, M. J., Perez-Leon, J., Wassle, H., and Backus, K. H. (2001). Characterization of the spontaneous synaptic activity of amacrine cells in the mouse retina. *Journal of Neurophysiology*, 86:1632–1643.

Hartline, H. K., and Ratliff, F. (1957). Inhibitory interaction of receptor units in the eye of Limulus. *Journal of General Physiology*, 40:357–376.

Hartline, H. K., and Ratliff, F. (1958). Spatial summation of inhibitory influences in the eye of limulus, and the mutual interaction of receptor units. *Journal of General Physiology*, 41:1049–1066.

Hartline, H. K., Wager, H., and Ratliff, F. (1956). Inhibition in the eye of limulus. *Journal of General Physiology*, 39:651–673.

Hubel, D. H., and Wiesel, T. N. (1962). Receptive fields, binocular interaction and functional architecture in the cat's visual cortex. *Journal of Physiology (London)*, 160:106–154.

Martinez, L. M., Alonso, J., Reid, R. C., and Hirsch, J. A. (2002). Laminar processing of stimulus orientation in cat visual cortex. *Journal of Physiology*.

Morgan, M. (1999). The poggendorff illusion: a bias in the estimation of the orientation of virtual lines by second-stage filters. *Vision Research*, 2361–2380.

Roska, B., Nemeth, E., and Werblin, F. (1998). Response to change is facilitated by a three-neuron disinhibitory pathway in the tiger salamander retina. *Journal of Neuroscience*, 18:3451–3459.

Stevens, C. F. (1964). *A Quantitative Theory of Neural Interactions: Theoretical and Experimental Investiga-tions*. PhD thesis, The Rockefeller Institute.

Tolansky, S. (1964). *Optical Illusions*. London: Pergamon.

Vogel, D. (2001). A biologically plausible model of associative memory which uses disinhibition rather than long-term potentiation. *Brain and Cognition*, 45:212–228.

Yu, Y., Yamauchi, T., and Choe, Y. (2004). Explaining low-level brightness-contrast illusions using disinhibition. In *Biologically Inspired Approaches to Advanced Information Technology (Bio-ADIT 2004; LNCS)*. New York: Springer. In press.